

NASA/TM—2007-214933

GT2006-91202



# Effects of Thermal Barrier Coatings on Approaches to Turbine Blade Cooling

*Robert J. Boyle*  
*Glenn Research Center, Cleveland, Ohio*

## NASA STI Program . . . in Profile

Since its founding, NASA has been dedicated to the advancement of aeronautics and space science. The NASA Scientific and Technical Information (STI) program plays a key part in helping NASA maintain this important role.

The NASA STI Program operates under the auspices of the Agency Chief Information Officer. It collects, organizes, provides for archiving, and disseminates NASA's STI. The NASA STI program provides access to the NASA Aeronautics and Space Database and its public interface, the NASA Technical Reports Server, thus providing one of the largest collections of aeronautical and space science STI in the world. Results are published in both non-NASA channels and by NASA in the NASA STI Report Series, which includes the following report types:

- **TECHNICAL PUBLICATION.** Reports of completed research or a major significant phase of research that present the results of NASA programs and include extensive data or theoretical analysis. Includes compilations of significant scientific and technical data and information deemed to be of continuing reference value. NASA counterpart of peer-reviewed formal professional papers but has less stringent limitations on manuscript length and extent of graphic presentations.
- **TECHNICAL MEMORANDUM.** Scientific and technical findings that are preliminary or of specialized interest, e.g., quick release reports, working papers, and bibliographies that contain minimal annotation. Does not contain extensive analysis.
- **CONTRACTOR REPORT.** Scientific and technical findings by NASA-sponsored contractors and grantees.

- **CONFERENCE PUBLICATION.** Collected papers from scientific and technical conferences, symposia, seminars, or other meetings sponsored or cosponsored by NASA.
- **SPECIAL PUBLICATION.** Scientific, technical, or historical information from NASA programs, projects, and missions, often concerned with subjects having substantial public interest.
- **TECHNICAL TRANSLATION.** English-language translations of foreign scientific and technical material pertinent to NASA's mission.

Specialized services also include creating custom thesauri, building customized databases, organizing and publishing research results.

For more information about the NASA STI program, see the following:

- Access the NASA STI program home page at <http://www.sti.nasa.gov>
- E-mail your question via the Internet to [help@sti.nasa.gov](mailto:help@sti.nasa.gov)
- Fax your question to the NASA STI Help Desk at 301-621-0134
- Telephone the NASA STI Help Desk at 301-621-0390
- Write to:  
NASA Center for AeroSpace Information (CASI)  
7115 Standard Drive  
Hanover, MD 21076-1320



# Effects of Thermal Barrier Coatings on Approaches to Turbine Blade Cooling

*Robert J. Boyle*  
*Glenn Research Center, Cleveland, Ohio*

Prepared for the  
Turbo Expo 2006  
sponsored by the American Society of Mechanical Engineers  
Barcelona, Spain, May 8–11, 2006

National Aeronautics and  
Space Administration

Glenn Research Center  
Cleveland, Ohio 44135

## Acknowledgments

The experimental data provided by Dr. Tony Arts and Dr. Karen Thole is greatly appreciated.

*Level of Review:* This material has been technically reviewed by technical management.

Available from

NASA Center for Aerospace Information  
7115 Standard Drive  
Hanover, MD 21076-1320

National Technical Information Service  
5285 Port Royal Road  
Springfield, VA 22161

Available electronically at <http://gltrs.grc.nasa.gov>

# Effects of Thermal Barrier Coatings on Approaches to Turbine Blade Cooling

Robert J. Boyle  
National Aeronautics and Space Administration  
Glenn Research Center  
Cleveland, Ohio 44135

## ABSTRACT

Reliance on Thermal Barrier Coatings(TBC) to reduce the amount of air used for turbine vane cooling is beneficial both from the standpoint of reduced NOx production, and as a means of improving cycle efficiency through improved component efficiency. It is shown that reducing vane cooling from 10% to 5% of mainstream air can lead to NOx reductions of nearly 25% while maintaining the same rotor inlet temperature. An analysis is given which shows that, when a TBC is relied upon in the vane thermal design process, significantly less coolant is required using internal cooling alone compared to film cooling. This is especially true for small turbines where internal cooling without film cooling permits the surface boundary layer to remain laminar over a significant fraction of the vane surface.

## Nomenclature

|           |                             |
|-----------|-----------------------------|
| $A$       | Area                        |
| $C_P$     | Specific heat               |
| $D$       | Leading edge diameter       |
| $d$       | Diameter of impingement jet |
| $G$       | Mass flux rate              |
| $h$       | Heat transfer coefficient   |
| $k$       | Thermal conductivity        |
| $M$       | Blowing ratio, $\rho V$     |
| $Nu$      | Nusselt number              |
| $Pr$      | Prandtl number              |
| $P$       | Vane pitch                  |
| $p$       | Hole pitch                  |
| $q$       | Heat flux                   |
| $Re$      | Reynolds number             |
| $Re_1$    | Unit Reynolds number        |
| $St$      | Stanton number              |
| $S$       | Surface distance            |
| $T$       | Temperature                 |
| $Tu$      | Turbulence intensity        |
| $t$       | Thickness                   |
| $V$       | Velocity                    |
| $w$       | mass flow rate              |
| $x, y, z$ | Hole spacing                |

|            |                               |
|------------|-------------------------------|
| $\alpha_2$ | Exit flow angle               |
| $\eta$     | Film effectiveness            |
| $\mu$      | Dynamic viscosity             |
| $\rho$     | Density                       |
| $\phi$     | Gas-to-wall temperature ratio |

## Subscripts

|      |                                |
|------|--------------------------------|
| 40   | Vane inlet                     |
| 41   | Vane exit                      |
| AW   | Adiabatic wall                 |
| C    | Coolant                        |
| CI   | Coolant inlet                  |
| CR   | Cross flow                     |
| EFF  | Effective                      |
| EXT  | Coolant extracted              |
| f    | Combustion                     |
| FILM | Film cooling                   |
| G    | Mainstream gas                 |
| I    | Coolant side                   |
| J    | Impingement jet                |
| M    | Metal                          |
| MI   | Coolant side metal temperature |
| O    | Exterior side                  |
| S    | Surface                        |
| TBC  | Thermal Barrier Coating        |
| TBCI | TBC interior                   |
| TBCO | TBC exterior                   |

## INTRODUCTION

The two primary reasons for reducing the fraction of compressor discharge air used for turbine vane cooling are the likelihood of reducing NOx production, and an improvement in component efficiency. Cycle efficiency is improved, without raising the rotor inlet temperature, by improvements in the component efficiencies. Reducing the amount of vane coolant air lowers the combustor outlet, (vane inlet), temperature, while maintaining a constant rotor inlet temperature. A lower vane inlet temperature should result in reduced NOx production. The desirability of NOx reduction for aircraft and especially ground power applications is widely recognized. NOx production is a very non-linear function of temperature[1]. Even a small reduction in combustion temperature can have a significant impact on NOx production.

Even though vane cooling air is described as non-chargeable air because it is available for work extraction in the rotor, there is a performance penalty to the vane. Because it is non-chargeable air, this cooling air often exceeds 10% of the main stream air. This high fraction of coolant air reduces vane efficiency. Reed and Turner[2] analyzed a two stage HP turbine, and presented their results as an entropy increase across each blade row. The entropy increase was divided into an aerodynamic loss and a mixing loss. The vane aerodynamic loss was due to boundary layer growth. The entropy increase due to mixing was strongly influenced by coolant flows. For the first stage vane, with a coolant flow rate of 9%, the entropy increase due to mixing was 119% of the aerodynamic entropy increase. For the second stage vane, with a coolant flow rate of only 2%, the entropy increase due to mixing was only 15% of the aerodynamic entropy increase. In addition, the broad cooled wakes associated with highly cooled vanes increase the unsteadiness seen by the rotor. Wilcock et al.[3], as well as MacArthur[4] point out that reductions in the required cooling fractions are needed before higher turbine inlet temperatures yield greater cycle efficiency.

Thermal Barrier Coatings(TBCs) have the promise of greatly reducing coolant flow requirements. However, they are subject to spallation. A conservative design approach is to design without relying on the insulating properties of the TBCs, and then apply them for their beneficial properties. Future improvements in TBC bond coats will reduce the likelihood of spallation. TBCs may then be relied on to reduce cooling flow rates. With reliance on TBCs the sensitivity of cooling flow rates to design parameters changes.

Arts et al.[5] showed that at moderate Reynolds numbers much of the suction surface of a solid vane remained laminar at an inlet turbulence of intensity of 6%. However, Arts[6] showed that just the presence of film cooling holes caused abrupt transition at the hole. A cooling scheme using only internal cooling, where the flow remains laminar, may be preferable to one using film cooling, where the flow transitions to turbulent near the leading edge.

Using only internal cooling is impractical when large amounts of cooling air have to be ejected from the trailing edge. To avoid an unacceptably thick trailing edge, current designs limit the coolant flow in this region to a few percent of the mainstream flow. The majority of the coolant is utilized as film cooling.

First, this paper illustrates the importance of reductions of turbine vane coolant as it relates to NOx production. Second, the paper examines the effects of utilizing TBCs on approaches to turbine vane cooling. In light of the reduced heat load associated with TBCs, the paper shows the conditions under which internal vane cooling alone may be preferred over film cooling. While most cooling schemes use a combination of both internal and film

cooling, the discussion focuses cooling the entire vane with only internal cooling or film cooling. Depending on the effectiveness level, film cooling often requires additional internal cooling in order to maintain acceptable vane temperatures.

In comparing internal only and film cooling several assumptions have to be made. To justify these assumptions several aspects of vane heat transfer are examined. Experimental and computational vane external heat transfer results are discussed. The choice of appropriate blowing ratios and film effectiveness values are examined. The sensitivity of required cooling to the fraction of cooling used for film cooling is analyzed. An impingement internal cooling scheme is chosen for comparing the required flow rates, because of its compatibility with two dimensional analysis. Finally, comparisons are shown for internal only and film cooling with and without TBC coatings at two vane Reynolds numbers.

## DISCUSSION of RESULTS

### NOx Reduction

NOx production is very sensitive to temperature, and it is very desirable to reduce NOx production. Reducing the combustor outlet temperature,  $T_{40}$ , substantially reduces NOx production. For a constant rotor inlet temperature,  $T_{41}$ , reducing the amount of vane coolant lowers the vane inlet temperature,  $T_{40}$ . By maintaining  $T_{41}$  constant, the turbine output power is unaffected.

Vane cooling air,  $w_C$ , often exceeds 10% of the main flow air. Rotor coolant air, which is chargeable air, since it does no work in the first stage, is generally less than 5% of  $w_{40}$ . Vane coolant air comes from the compressor discharge at a temperature,  $T_C$  approximately half of the vane outlet temperature,  $T_{41}$ . A constant  $C_P$  heat balance gives:

$$T_{41} = \frac{T_{40}}{1 + w_C/w_{40}(1 - T_C/T_{41})}$$

Shuman[7] showed NOx production as a function of temperature for different combustors. This reference showed that the slopes of the lines for different combustors are similar. Mello et al.[8] gives a rate of NOx production as:

$$NOx = Cexp(-a/T)$$

where  $a = 23650^\circ K$ , and the constant  $C$  incorporates other combustor parameters.

Tacina et al.[9] correlated NOx production as a function of fuel-to-air ratio, combustor inlet temperature,  $T_3$ , pressure,  $P_3$ , pressure drop,  $\Delta P/P_3$ , The combustor inlet temperature,  $T_3$ , equals the coolant temperature,  $T_C$ . The

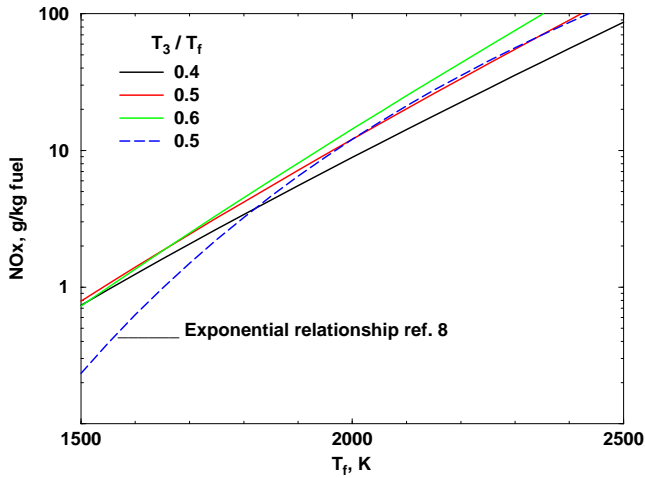
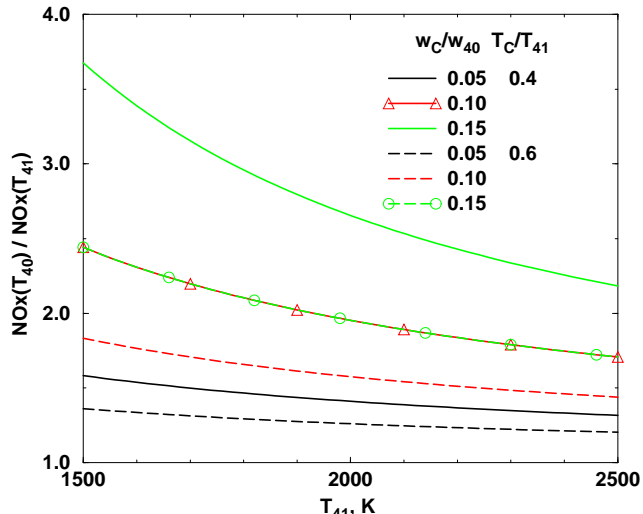
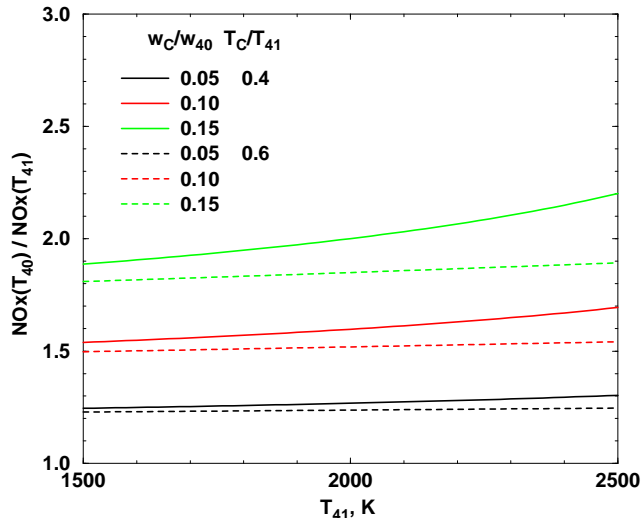


Fig. 1 NOx production for  $P_3 = 2760kPa$ ,  $\Delta P/P_3 = 3\%$ .



a) Reference 8 correlation



b) Reference 9 correlation

Fig. 2 Ratio of NOx production with vane coolant to NOx production with no coolant

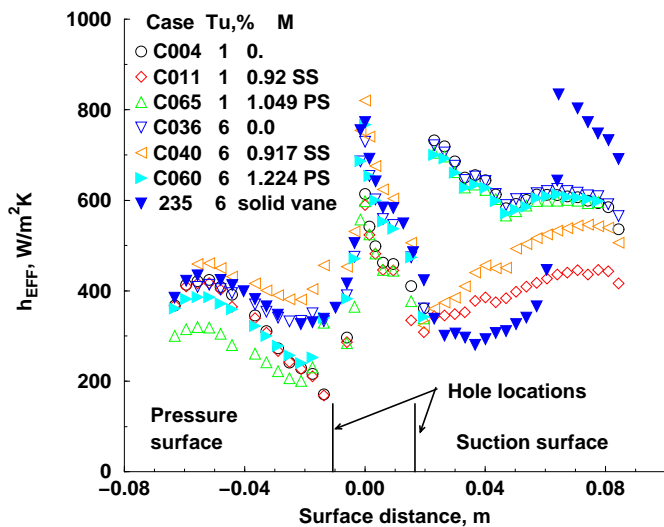
combustion temperature,  $T_f$ , was found by assuming a fuel-to-air ratio, and Jet-A fuel properties. Figure 1 shows the NOx production as a function of  $T_f$ , and  $T_3/T_f$  using the correlation of reference 9 that best agrees with their data in the neighborhood of  $2000^\circ K$ . In this correlation the exponent for the fuel-to-air-ratio was 3.88. The effect of variations in  $T_3/T_f$  is relatively minor. Increasing  $T_3$  at constant fuel-to-air ratio, increases NOx production. But, increasing  $T_3$  at constant  $T_f$  decreases the fuel-to-air ratio, which tends to offset the NOx production due to increased  $T_3$ .

Figure 1 also shows the NOx production for natural gas combustors using the relationship of reference 8. This paper's focus is on the change in NOx production with temperature, and not on the absolute NOx level. The constant,  $C$ , in the above equation from reference 8 was chosen to give the same NOx level as that of reference 9 at  $T_f = 2000^\circ K$ , and  $T_3/T_f = 0.5$ . Even though the curves are derived from different sources, the slopes in the high temperature region are similar.

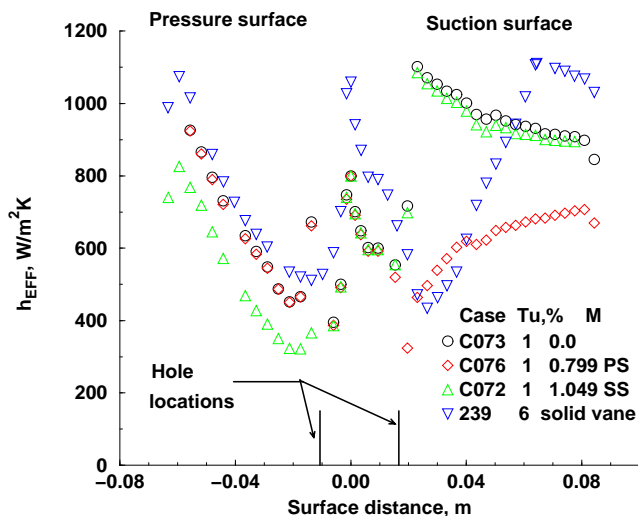
Figure 2 shows the ratio of NOx production with vane coolant,  $NOx(T_{40})$ , to NOx production without vane coolant,  $NOx(T_{41})$ . Curves are shown for two vane coolant to vane exit temperature ratios, and for three coolant to main stream flow rate ratios. These curves were generated assuming  $T_{40} = T_f$ . In practice  $T_{40}$  is less than  $T_f$  due to combustor cooling. Tacina et al.[9] state that combustor cooling should be on the order of 10% of the mainstream flow. Calculations of NOx production, which accounted for combustor cooling, gave almost the same ratios as are shown in figure 2.

Figure 2a shows ratios determined using the correlation of reference 8, where the ratio of NOx production is  $exp(-a/T_{40})/exp(-a/T_{41})$ . While the ratio of NOx production goes down with increasing  $T_{41}$ , the actual NOx production increases rapidly with temperature. At  $T_{41} = 2000^\circ K$  a reduction of 0.05 in the coolant flow rate gives a reduction in NOx of over 25% at  $T_c/T_{41} = 0.4$ , and of nearly 20% at the higher coolant temperature ratio.

Figure 2b shows ratios determined using the correlation of Tacina et al.[9]. Except that the ratio is less sensitive to  $T_{41}$ , the results at high temperatures are similar in the two figures. The much steeper slope at low  $T_{41}$  values shown in figure 1 for the relationship of reference 8 is the reason why the NOx production ratio is greater at low temperatures in figure 2a than in figure 2b. Reducing the coolant flow rate lowers NOx production. A reasonable goal is to reduce  $w_c$  from 10 to 5% of  $w_{40}$ . Both parts of figure 2 show that this could result in a 25% reduction in NOx. Improved combustor designs will result in lower NOx production. But, due to its sensitivity to combustion temperature, NOx production will remain sensitive to the vane coolant flow rate ratio.



a) True chord exit Reynolds No. =  $1 \times 10^6$



b) True chord exit Reynolds No. =  $2 \times 10^6$

Fig. 3 Net heat transfer coefficient - data of Arts[6]

### Comparison of film and internal cooling

External heat transfer data. Experimental data show that just the presence of film cooling holes causes a tripping of a laminar boundary layer to turbulent. At low Reynolds numbers this can result in large relative heat transfer increases. Figure 3 illustrates this. The data from Arts et al.[5], for a solid vane, and from Arts[6], for the same vane with cooling holes are shown. In the experiments of Arts[6] there were two rows of closely spaced film cooling holes on both the pressure and suction surface. The suction surface coolant rows were at surface distances of 0.0166 and 0.0186 meters. On the pressure surface the distances were

-0.0107 and -0.0134 meters. The symbols for case 235 are for the solid vane at an inlet turbulence intensity of 6%. C036 data are for the same turbulence intensity, and no flow through the cooling holes. These data show a rapid increase in suction surface heat transfer near the cooling holes. The effect of tripping the boundary layer is strongly dependent on Reynolds number and turbulence level. On the pressure surface, where the local Reynolds number is lower, there is not a significant heat transfer increase at the cooling holes. For the case shown, the average heat transfer increase for the suction surface downstream of the holes is nearly 30%, even though the solid vane heat transfer is higher after transition.

Also shown in figure 3a are experimental data for blowing ratios close to one. To prevent hot gas ingestion in engine applications the cooling plenum total pressure exceeds the gas side total pressure. Therefore, local blowing ratios are typically one or greater. Tests were conducted with either suction(SS) or pressure(PS) side blowing, but not both simultaneously. Here  $h_{EFF}$  is the effective heat transfer coefficient, which accounts for the effects of film cooling, and is proportional to the heat transfer rate.  $h_{EFF} = q/(T_G - T_S)$  Comparing the 1% and 6% turbulence intensity results show that high inlet turbulence reduces the benefits of film cooling. The C040 results show a noticeable increase in pressure side heat transfer, as a result of suction surface blowing. This implies that suction surface blowing upstream of the throat increases freestream velocities near the pressure surface.

Figure 3b shows the experimental data for a Reynolds number of  $2 \times 10^6$ . The solid vane transitions at about the same location as the film cooled vane. On the suction surface the transition length is longer, even though the turbulence intensity is greater. There is no film cooling in the leading edge region. In this region, and on the pressure surface the heat transfer is lower. Without any coolant the lower turbulence causes lower heat transfer in both the leading edge region, and on the pressure surface. When cooling is present the heat transfer is lower on both the suction and pressure surfaces. However, based on the results in figure 2a, the heat transfer reduction would be less if the inlet turbulence were higher.

The appropriate Reynolds number for comparisons is largely determined by the size of the vane. Many modern turbines are designed for an inlet pressure near 35 atmospheres, and a temperature near  $2000^\circ K$ . Since  $\rho V$  is a maximum at sonic conditions, a vane row exit Reynolds number is relatively insensitive to the vane pressure ratio. For these conditions the unit Reynolds number,  $(\rho V/\mu)$  is approximately  $500000 cm^{-1}$ . A small aircraft or micro turbine, with an axial chord of 1 cm, and a true chord of 2 cm, has a vane true chord exit Reynolds number of nearly a million. The Reynolds number could be several million



for large aircraft or ground power turbines. At cruise an aircraft engine vane Reynolds number is reduced by about a factor of three. A moderate size aircraft engine at cruise, or a small ground power engine has true chord vane exit Reynolds numbers in the one-to-two million range.

References 5 and 6, and references 10 to 12 show experimental vane heat transfer at moderate to high turbulence levels. Average suction surface exit Stanton numbers were in the range  $0.001 < St < 0.002$ . Nealy et al.[10] measured midspan average suction surface Stanton number of 0.0013 and 0.0016 for two vane geometries at exit true chord Reynolds numbers of  $2.5 \times 10^6$ . Inlet turbulence intensities were 6 to 8 percent. Radomsky and Thole[11] measured average suction surface midspan vane Stanton numbers of 0.0020 and 0.0022 for an exit Reynolds number of  $1.1 \times 10^6$ , and turbulence intensities of 10 and 20%. They also showed  $St \propto Re^{-0.2}$ . Adjusting the Stanton numbers of reference 11 to the Reynolds number of reference 10 gives Stanton numbers of 0.0019 and 0.0017. Harasgama and Wedlake[12] measured full span vane heat transfer over a range of Reynolds numbers, and an inlet turbulence intensity of 6.5%. At their highest Reynolds number of  $5.2 \times 10^6$  the average midspan suction surface Stanton number was 0.0012. This midspan suction surface Stanton number was greater than the spanwise average for the suction surface. Correcting the 0.0012 value to the Reynolds number of reference 10 increases it to 0.0014.

These references generally show average pressure surface Stanton numbers about 80% of the average suction surface value. An exception is the data of Harasagama and Wedlake[12]. Their high Reynolds number data showed that the average pressure and suction surface heat transfer rates were nearly equal, due to pressure surface transition very close to the leading edge.

A Stanton number of 0.001 gives a reasonable approximation for the entire vane surface. For a gas temperature of  $2000^\circ K$ , and a unit Reynolds number of  $500000 cm^{-1}$ , a Stanton number of 0.001 corresponds to a heat transfer coefficient of  $4340 W/m^2 K$ .

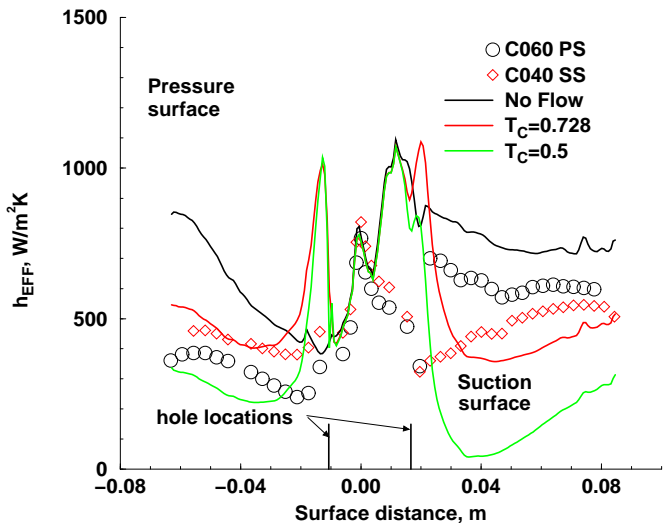
Leading edge region data show much larger variations in heat transfer coefficients. Heat transfer in the leading edge region can be determined from  $Nu_D = C\sqrt{Re_D}$ .  $C$  is about 1.4 to account for high turbulence levels.  $Re_D$  is the inlet Reynolds number based on the leading edge diameter,  $D$ .  $Re_D$  can vary by more than a factor of ten between small and large engines. The external heat transfer coefficient,  $h_O$ , is proportional to  $\sqrt{Re_D}/D$ . The inlet-to-exit Reynolds number ratio changes with the exit flow angle, and the diameter-to-chord ratio varies among different design approaches. Giel et al.[13] showed that for a high  $Re_D = 2.1 \times 10^5$ , and a turbulence level near 8%, the peak leading edge heat transfer had a corresponding exit Stanton number of 0.0025. The average over the leading edge region was less than 0.002.

Leading edge film cooling heat transfer rates and effectiveness strongly depend on the turbulence level. The blowing ratio is typically given as the ratio of the local mass flux to the inlet mass flux. In practical applications this value is likely to be close to one, in order to avoid hot gas ingestion. Ekkad et al.[14] measured heat transfer coefficients and effectiveness values on a leading edge cylindrical model for different turbulence intensities and density ratios. For an included angle of  $\pm 70^\circ$ , the average heat transfer increased linearly with the coolant momentum flux ratio. At their highest turbulence intensity of 7%, the increase was 50% at a momentum flux ratio of 1.5. For momentum flux ratios between 1 and 1.5 the effectiveness was between 0.12 and 0.14.

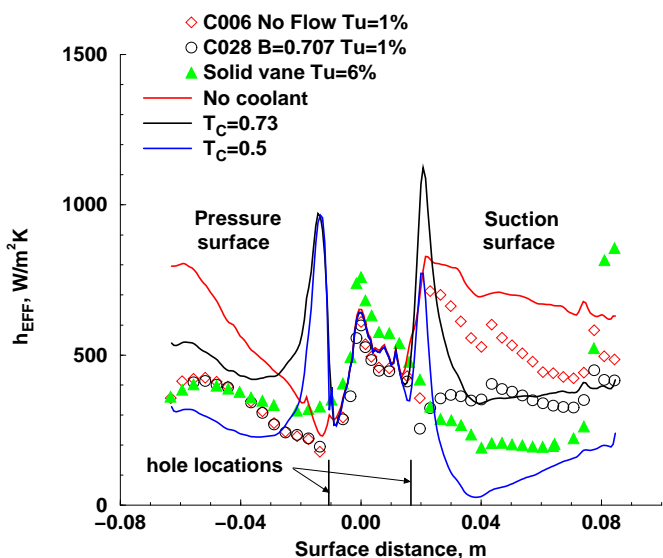
External heat transfer predictions. CFD calculations for heat transfer distributions on a film cooled vane or rotor blade are more complex than those for a solid blade. This is especially true when the calculations include the cooling hole and plenum geometries. Garg[15] gave results for several comparisons for film cooled blade heat transfer. Several of these comparisons were made using the NASA GlennHT 3D Navier-Stokes code described by Steinhilber et al.[16]. This code is a generalized multiblock finite volume code.

Figure 4 compares CFD predictions using the GlennHT code with the data of Arts[6] for true chord exit Reynolds numbers of 1 and 2 million. The computational domain was the midspan section of the vane. Symmetric boundary conditions were applied in the spanwise direction. In addition to the main stream flow path, the plenums, and the cooling passages within the vane were incorporated into the CFD model. Calculations were done with either no coolant air or with flow from both plenums simultaneously.  $T_C/T_G$  ratios of 0.728 and 0.5. The value of 0.728 corresponds to the experimental data, and the value of 0.5 is more typical of actual engine applications. The data were obtained with blowing from only one of the two plenums during each test. Thus, in figure 4a, the C040 data are for suction side blowing, but no pressure side blowing. The C060 data are for pressure side blowing, but no suction side blowing. Comparisons are shown for blowing ratios that are either zero or close to one. Near the cooling holes there is a sharp spike in the predicted pressure side heat transfer. On the suction side the data show a heat transfer rise consistent with tripping the boundary layer just due to the presence of the cooling holes.

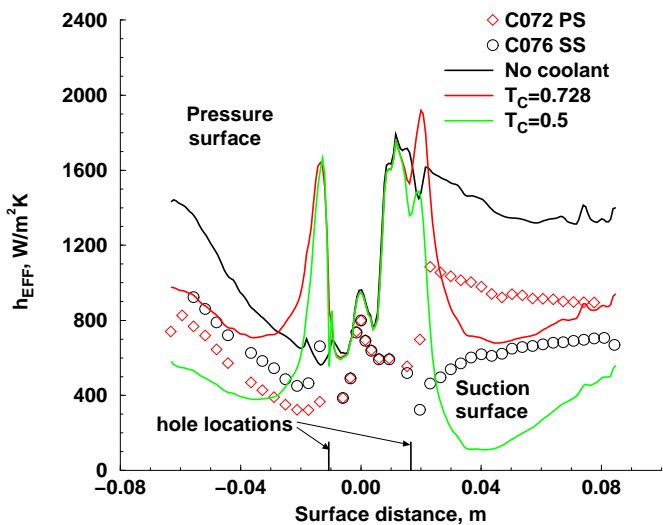
For all three parts of figure 4, the fully turbulent heat transfer prediction exceeds the pressure surface data. However, for the rear half of the pressure surface the change in heat transfer with film cooling is reasonably well predicted. At  $Re = 1 \times 10^6$  the leveling off of the experimental pressure surface heat transfer may be due to a relaminarization effect, which is not captured in the turbulence modeling.



a) True chord exit Reynolds No. =  $1 \times 10^6$ ,  $M_2 = 0.9$



b) True chord exit Reynolds No. =  $1 \times 10^6$ ,  $M_2 = 1.1$



c) True chord exit Reynolds No. =  $2 \times 10^6$ ,  $M_2 = 0.9$

Fig. 4 Comparison of heat transfer predictions with data

However, at the higher Reynolds number there is no evidence of relaminarization in the data, and the prediction is still higher than the data. Comparisons are made matching the experimental blowing ratio. The analysis gave a smaller discharge coefficient than the data, and for the same plenum pressure the calculated cooling flows were lower than the experimental flows. On the pressure surface, lower coolant flows reduced the peak heat transfer just downstream of the coolant holes, but increased the heat transfer for the remainder of the pressure surface. The peak in pressure surface heat transfer is not seen in the data. Conduction within the vane, which was not considered in the analysis, may be partially responsible for the lack of a corresponding peak in the experimental data. In the leading edge region the predictions agree with the data. The predictions show early suction surface transition when either the inlet turbulence is high, 6% in figure 4a, or when the Reynolds number is high,  $2 \times 10^6$  in figure 4c. If film cooling is not used in the leading edge region, accurate transition predictions are needed in the turbulence modeling.

Comparisons between predictions and data for the suction surface show that early transition may be somewhat responsible for the the high heat transfer prediction. Downstream of the cooling holes the predicted level is too high, but in figures 4a and 4c the change in heat transfer with distance is well predicted. Predictions show larger than measured decreases in heat transfer with film cooling. In figure 4b the film cooled suction surface heat transfer prediction agrees well with the data. In figure 4a the prediction is lower than the data, and in figure 4c the prediction is higher. Overall, the agreement is reasonably good.

Figure 4b shows that the benefits of not tripping the boundary layer can approach the benefits of film cooling without the penalty of added cooling air. The solid symbols are for the solid vane, and are at a higher inlet  $Tu$  of 6%. The exit Mach number,  $M_{2m}$  is than in figure 4a, and the suction surface pressure gradients are more favorable. For the solid vane transition is suppressed until a distance of over 0.06m. At this location the film cooled prediction with  $T_C/T_G = 0.5$  has only a slightly lower heat transfer than the solid vane. The No-Flow heat transfer data also show the effects of a more favorable pressure gradient. Figures 4a and 4b show nearly the same peak suction surface heat transfer just downstream of the cooling holes, but the stronger favorable pressure gradient at the higher Mach number results in a significantly lower heat transfer for the remainder of the suction surface. The tests were done for vanes with constant span. Engines typically have converging endwalls, which strengthen the favorable pressure gradients. The converging endwalls effectively move the loading further aft on the vane. Schiele et al.[17] measured vane heat transfer over a range of Reynolds numbers and turbulence intensities for an aft loaded vane at an exit chord Reynolds number over 900,000, suction surface transition

did not occur upstream of the throat, even when the inlet turbulence intensity was 13.5%. They attributed the delay of transition to the favorable pressure gradient, which was a consequence of the aft loading. Approaches to predicting transition, as well as heat transfer augmentation due to high freestream turbulence have been discussed by Boyle et al.[18] and others.

The calculations with  $T_C/T_G = 0.5$  show that the heat transfer approaches zero only near the suction surface distance of 0.04m . Even near the pressure surface cooling holes, and downstream of the cooling holes on both the pressure and suction surfaces, substantial internal cooling is required to maintain a surface temperature less than the gas temperature.

While the overall agreement between analysis and data is not as good as one would like, the predictions show the correct trends. To verify that the disagreements were due to modeling assumptions, and not to grid effects, check cases were run. Changes in the near wall grid spacing, at a near constant spacing ratio, resulted in no significant heat transfer differences. The predictions shown in figure 4 are with the finer grid spacing, with first node near wall  $y^+$  spacing much less than one. Because of the high pressure surface heat transfer near the coolant holes, the manner in which the coolant entered the plenum was varied. At the same blowing ratios, the heat transfer was nearly identical.

Vane loss calculation. The average loss in total pressure was calculated for three of the predictions shown in figure 4b. When there was flow out of the coolant holes at the experimental temperature, the total pressure loss increased by 8 %. This increase was caused by a total coolant flow rate of only 1.8% of the mainstream flow. There was an additional loss increase of one percent when  $T_C/T_G$  was reduced to 0.5. Lowering the coolant temperature increases the coolant mass flow rate. Extrapolating these results to high coolant flow rate ratios shows nearly a forty percent increase in total pressure loss due to a ten percent coolant-to-mainstream flow rate ratio.

Film cooling blowing ratio. The ratio of film cooling to mainstream flow is given by:

$$\frac{w_{C-FILM}}{w_{40}} = \frac{\pi d_C^2}{4Pp} \sum_{i=1}^{N_{rows}} (M_{REF})_i$$

where  $P$  is the vane pitch,  $p$  is the cooling hole pitch in the spanwise direction, and  $N_{rows}$  is the number of rows. This shows that the cooling hole diameter,  $d_C$ , should be as small as practical, even when  $p/d_C$  remains constant.  $M_{REF}$  is the reference blowing ratio, and is given by:

$$M_{REF} = \frac{(\rho V)_{INLET}}{(\rho V)_{LOCAL}} M_{LOCAL}$$

Average film cooling effectiveness. Since the coolant hole total pressure should exceed the freestream total pressure, and the cooling temperature is about half of the freestream temperature, ideal  $M_{LOCAL}$  values approach two. Because of entrance losses, practical blowing ratios are near one.

To minimize film cooling usage the number of film cooling rows and the size of the holes should be as small as possible. This leads to widely spaced rows of holes. The film cooling configuration of Arts[6] had pressure and suction surface lengths downstream of the cooling holes of 100 and 140 hole diameters. Other than near the leading edge, the mid point of the distance covered by film cooling is often on the order of 50 diameters. There are many film cooling studies, references 18 to 20 for example, which show that the average effectiveness over a distance of 100 hole diameters is approximately 0.1. Bons et al.[19] showed that the high effectiveness close to the cooling holes for a low blowing ratio of 0.75 is greatly diminished by high freestream turbulence. With a turbulence intensity of 17% the effectiveness 50 diameters from the cooling hole was reduced to 0.05. This reference showed a smaller decrease in film effectiveness due to turbulence at a blowing ratio of 1.5. At 50 hole diameters the effectiveness increased to 0.08. For a turbulence intensity of 1% the effectiveness at 50 hole diameters was close to 0.14 at either blowing ratio. Takeishi et al.[20] showed turbine vane suction surface effectiveness values near 0.14 at 50 hole diameters. Pressure surface effectiveness was even lower, being 0.04 at 50 diameters. These results are very similar to those reported by Drost and Bolcs[21]. Higher average effectiveness values are sometimes reported. However, these are for either low blowing ratio, or in the presence of low turbulence.

Sensitivity to internal heat transfer. For film cooling the ratio of heat transfer with film cooling to heat transfer without film cooling,  $q_{RATIO}$ , is given by:

$$q_{RATIO} = \frac{q_{FILM}}{q_{NO-FILM}} = \frac{h_{FILM}}{h_{NO-FILM}} \left(1 - \frac{\eta}{\phi}\right)$$

If  $\eta/\phi$  is at least one, no internal cooling is needed, and the only requirement is to provide sufficient cooling to achieve the desired value for  $\eta$ . The two parameters  $\phi$ , and  $\eta$  are given by:

$$\phi = (T_G - T_S)/(T_G - T_C)$$

$$\eta = (T_G - T_{AW})/(T_G - T_C)$$

$T_S$  increases for designs relying on TBCs relative to designs which do not rely on the insulating properties of TBCs. If  $1 - \eta/\phi$  is less than zero, there is no need for internal cooling. However, at high turbulence levels the average value for  $\eta$  is low, so that internal cooling may still be required when TBCs are used.

Table I. Values used in analysis

|  | Inconel | TBC   |
|--|---------|-------|
| Conductivity, $k, W/mK$                | 31.0    | 1.0   |
| Reference                              | 22      | 23    |
| Thickness, $t, mm$                     | 1.5     | 0.3   |
| $k/t, W/m^2K$                          | 20700   | 3333  |
| Heat transfer coefficient, $h, W/m^2K$ | 4500    | 4500  |
| $h/(k/t)_{METAL}$                      | 0.217   | 0.217 |

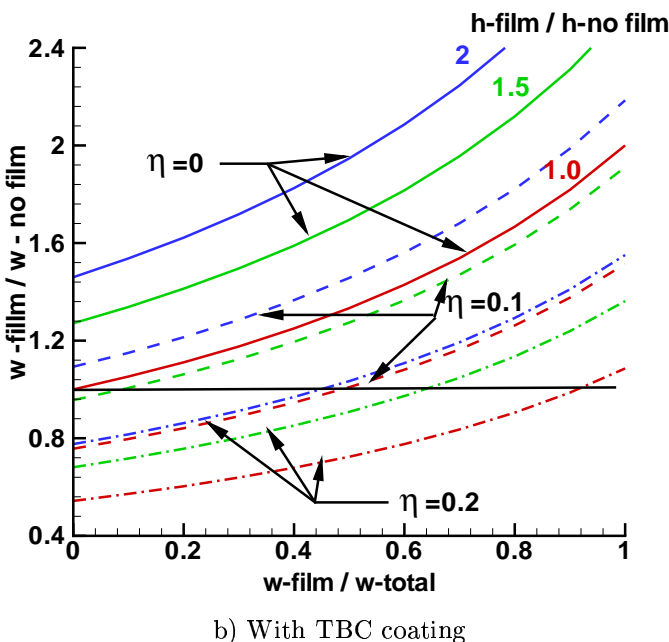
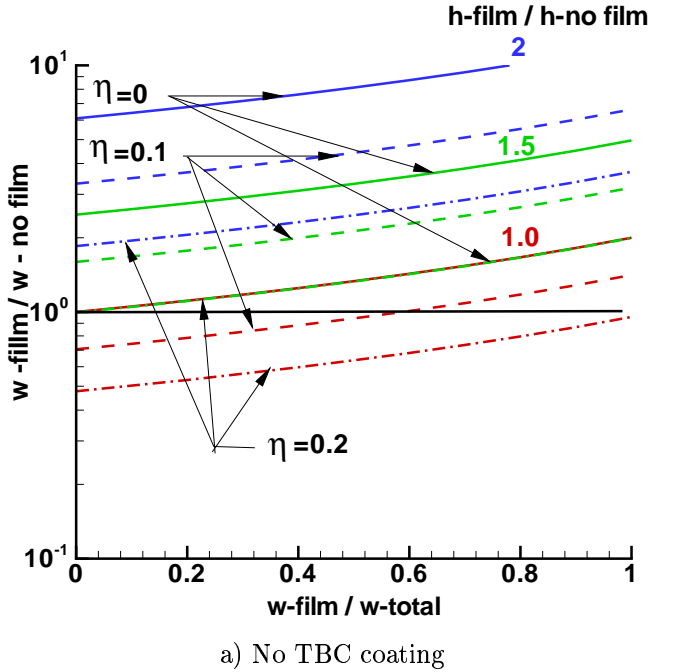


Fig. 5 Increase in cooling flow due to extraction.

As coolant air is withdrawn from the blade, there is less coolant available for internal cooling. Han, Dutta, and Ekkad[22] show that for a variety of internal cooling arrangements the Nusselt number is proportional to the Reynolds number to a power,  $n$ . This exponent is generally between 0.65 and 0.75. The local coolant flow rate is proportional to the Reynolds number. If all of the coolant is used for film cooling, the average Reynolds number is half the inlet value. Consequently, the average internal heat transfer is reduced by nearly 40%.

Figure 5 illustrates the effect of withdrawing coolant on the amount of coolant required to maintain a constant maximum metal temperature. These results are for a coolant-to-gas temperature ratio of 0.5, and a maximum metal temperature-to-gas temperature ratio of 0.7. Also this figure was determined using nominal values for Inconel and TBC thermal conductivities[23 and 24], and thicknesses[25]. They are given in Table I. This table also includes a mid-range value for the external heat transfer coefficient. Variations in the properties shown in Table I resulted in figures similar to figure 5. Appendix A gives the details of the calculations used to generate figure 5.

The positive slopes of the curves in figure 5 result from lower internal heat transfer as the fraction of total coolant used for film cooling is increased. Even though with film cooling the effective heat transfer coefficient,  $h_{EFF}$ , is generally lower than the actual heat transfer coefficient,  $h_O$ , Film cooling increases  $h_O$  compared to no film cooling. This increase can be substantial, if film cooling causes a laminar boundary layer to become turbulent.

Comparing figures 5a and 5b shows that the coolant flow ratio is less sensitive to  $h$  variations when the TBC coating is present. The relationship between  $\eta$  and  $h$  is illustrated in this figure. With a TBC coating an  $\eta = 0.2$  and a  $h_{FILM}/h_{NOFILM} = 2$  gave the same results as when  $\eta = 0.1$  and the heat transfer ratio was 1.0. Both parts of figure 5 show that even if the heat transfer ratio is 1, but nearly all the coolant is used for film cooling, there is no reduction in required coolant for  $\eta$  values less than 0.2. Even though the decrease in  $\eta$  with distance from the cooling holes is to some extent compensated by  $h_{FILM}/h_{NOFILM}$  approaching one, there is a significant increase in required coolant if a substantial fraction of the coolant is used for film cooling.

Figure 5 does not account for any increase in the average coolant temperature for either film or non-film cooled vanes. For flow in the spanwise direction, and no film cooling the average coolant temperature increases as the flow progresses. With film cooling there is a decrease in the flow rate as the flow progresses. Either way, the internal heat transfer increases to accommodate the rise in the coolant temperature. This can be shown by equating the heat load based on the inlet coolant temperature,  $T_{CI}$ , and a required internal heat transfer coefficient,  $h_{I-REQ}$  with the one based on the average coolant temperature,  $T_C$ , and the actual heat transfer coefficient,  $h_I$ . Equating the

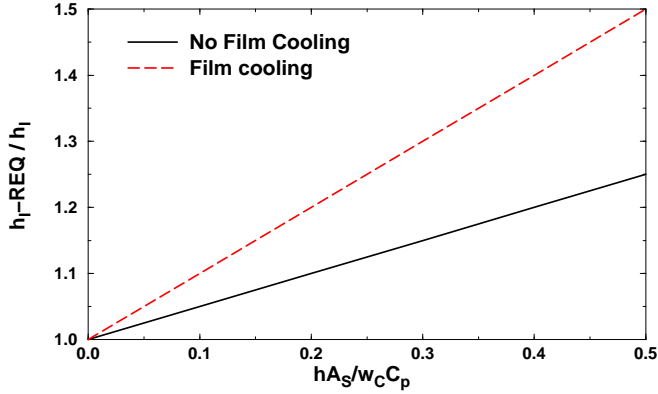


Fig. 6 Increase in cooling required due to fluid heating.

internal heat load gives:

$$\frac{h_{I-REQ}}{h_I} = \frac{(T_{MI} - T_{CI})}{(T_{MI} - \overline{T_C})} = 1 + \frac{(\overline{T_C} - T_{CI})}{(T_{MI} - \overline{T_C})}$$

For no film cooling:

$$\overline{T_C} = T_{CI} + h_I A_S (T_{MI} - \overline{T_C}) / (2w_C C_P)$$

where  $A_S$  is the surface area of the vane. In terms of the heat transfer ratio this becomes:

$$h_{I-REQ}/h_I = 1 + h_I A_S / (2w_C C_P)$$

With all cooling going to film cooling the average flow rate is reduced by half, so that the rise in coolant temperature doubles. Then:

$$h_{I-REQ}/h_I = 1 + h_I A_S / (w_C C_P)$$

The term  $h_I A_S / w_C C_P$  can be estimated by assuming a spanwise oriented cylinder heated over half its surface area. Cooling channels have internal Stanton numbers about 0.010. A channel has a length-to-diameter ratio near 10. Using these values gives  $h_I A_S / w_C C_P = 0.2$ . A rectangular cooling channel with a width to vane span ratio of 0.05 gives the same value for  $h_I A_S / w_C C_P$ .

Figure 6 shows the required heat transfer ratio for all film cooling and no film cooling. While film cooling has a higher slope, the effect of accounting for the increased cooling temperature is expected to be small.

Other internal cooling approaches can have  $h_{I-REQ}/h_I$  more independent of  $h_I A_S / w_C C_P$ . If impingement cooling is used in conjunction with all film cooling, the inlet and local values of  $T_C$  are the same.

**Internal heat transfer.** To compare the change in cooling flows due to TBCs and film cooling, calculations were made using an impingement heat transfer scheme. Of the several approaches for internal cooling available, this approach is taken because it addresses the relevant internal cooling NASA/TM—2007-214933

issues, and is suitable for a two dimensional analysis. This scheme also has similarities to film cooling heat transfer. The correlation given by Florschuetz et al.[26] for a staggered array of holes is used. With no cross-flow the Nusselt number based on jet diameter,  $d$  is:

$$Nu_{dNC} = 0.363(x/d)^{-0.554}(y/d)^{-0.422}(z/d)^{0.068} Re_d^{0.727} Pr^{1/3}$$

where  $z/d$  is the normalized distance to the surface.  $x/d$  and  $y/d$  are the pitches of the holes. For simplicity,  $x/d$  is assumed equal to  $y/d$ .

With cross-flow the Nusselt number is reduced by:

$$Nu_d = Nu_{dNC} \left( 1 - Cr(x/d)^{Nx} (y/d)^{Ny} (z/d)^{Nz} (G_{CR}/G_J)^{NG} \right)$$

$G_{CR}$  and  $G_J$  are the mass fluxes for the cross-flow and jet respectively. In-line impingement holes have a lower cross-flow penalty than do staggered impingement holes. For in-line holes  $Cr = 0.596$ ,  $Nx = -0.103$ ,  $Ny = -0.38$ ,  $Nz = 0.803$ , and  $NG = 0.561$ .

Without cross-flow the Nusselt number is relatively insensitive to the wall-to-jet spacing,  $z/d$ . However, the cross-flow reduction is strongly influenced by this ratio. Exclusive of upstream cross flow,  $z/S$  times  $G_{CR}/G_J$  is proportional to the total cross flow-to-jet flow ratio, with  $S$  being the length of the impinged surface.

Using the relationship for the internal Stanton number that  $St_I = Nu_d / Re_d Pr = h_I A / w_C C_P$ , a figure of merit can be defined. This figure of merit is the heat transfer coefficient divided by the coolant flow rate per unit surface length and span. It is given by:

$$\frac{h_I A_S}{w_C} = \frac{4 Nu_d C_P}{\pi Re_d Pr} \left( \frac{x}{d} \right)^2$$

Figure 7 shows  $h_I A_S / w_C$  for the no cross-flow case as a function of the unit Reynolds number for the jet,  $Re_1 = Re_d / d$ . As the ordinate increases, the required coolant flow decreases for a given value of  $h_I$ . The unit Reynolds number of the jet is related to the external unit Reynolds number, since both have nearly the same total pressure. If the jet Mach number is 0.25, and the coolant-to-gas temperature ratio,  $T_C / T_G$ , is 0.5, the coolant unit Reynolds number is about half of the mainstream unit exit Reynolds number. For these assumptions the coolant unit Reynolds number is about  $250,000 cm^{-1}$ . The figure of merit is not a strong function of  $z/d$ , and a  $z/d = 5$  is used. Curves are shown for hole diameters, 0.5mm, 1.0mm, and 2.5mm. As the hole diameter decreases  $h/w_C$  increases. Not surprisingly, small diameter holes give better figures of merit. The implication in this figure is to use the small values for  $d$ , and  $Re_1$ , and large values for  $x/d$ . However, they cannot be arbitrarily chosen.  $h_I$ , which depends on these parameters, must be large enough to achieve the desired maximum material temperature.

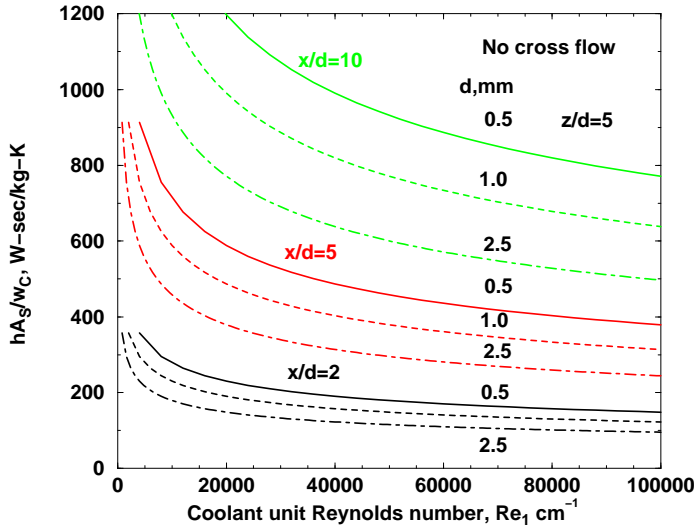


Fig. 7 Sensitivity of coolant to geometry parameters.

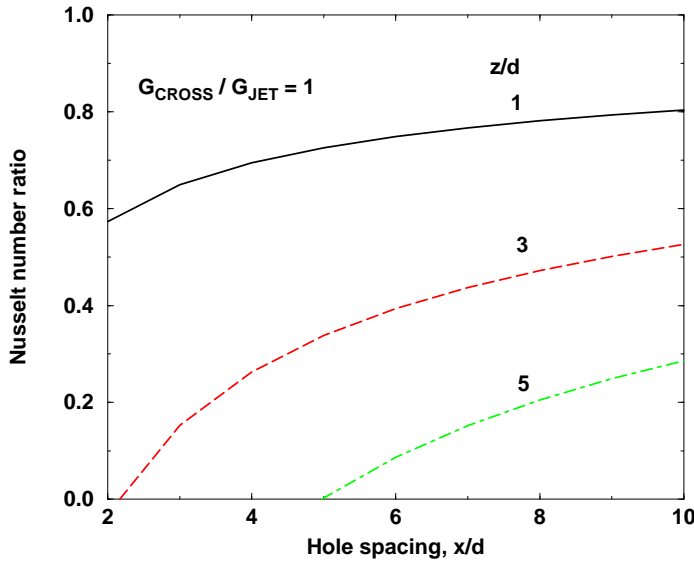


Fig. 8 Effect of cross flow on required coolant flow.

Figure 8 shows the cross-flow effect on Nusselt number for  $G_{CR}/G_J = 1$ , and illustrates the limitations of internal only cooling. Small  $z/d$  values are needed to minimize the heat transfer reduction due to cross flow. However, small  $z/d$  values result in large coolant pressure drops unless the hole spacing,  $x/d$  is large. Maximizing  $x/d$  minimizes the reduction in heat transfer due to cross flow. When all the internal cooling is used for film cooling, there is no cross flow. When no film cooling is used, the mass flux ratio approaches one, and can significantly reduce the internal  $h$ .

Figure 8 shows  $Nu_d$  going to zero at different combinations of  $x/d$  and  $z/d$  values. This is due to extrapolation of the correlation beyond its data base. Florschuetz et al.[25] showed results where the ordinate in figure 8 was greater NASA/TM—2007-214933

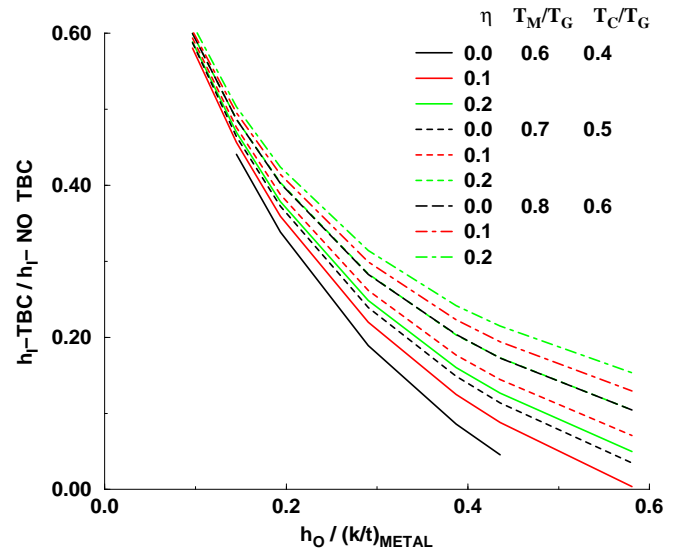


Fig. 9 Effect of TBC on required  $h_I$ .

greater than 0.4. It initially seemed appropriate to base a minimum Nusselt number on channel flow using the cross flow mass flux,  $G_{CR}$ . However, this approach has the heat transfer increasing with increasing  $G_{CR}$ , in contradiction to the experimental data.

Heat transfer comparisons are made assuming the entire vane is cooled using jet impingement cooling. It is recognized that impingement is not practical in the aft portion of the vane, where a pin fin arrangement may be needed. However, it is felt that, whatever internal cooling approach is used, that the relative effects of relying on a TBC on the choice of using internal only or film cooling would be similar.

Benefits of TBCs. Because of the low conductivity of the TBCs, the heat flux is greatly reduced. For a constant maximum metal temperature the temperature decrease across the metal is less with TBCs. Consequently, the wall-to-coolant temperature difference is larger, and less internal coolant is required. This is illustrated in figure 9, where the ratio of internal cooling with TBCs to internal cooling without TBCs is given as a function of the normalized external heat transfer coefficient. Figure 9 shows why film cooling is presently used. When the ordinate ratio goes to zero, the inner wall temperature is the same as the coolant gas temperature for a metal only blade, and an infinite amount of cooling is required. With film cooling the curves shift to the right as  $\eta$  increases. When  $\eta$  increases sufficiently, only a reasonable amount of cooling is needed. As  $h_O$  decreases, the ratio of  $h_I$  with and without TBCs approaches one. If the external heat flux is very low, the required internal cooling is low, and is less affected by the presence of a TBC. Increasing  $\eta$ , reduces  $h_{O-EFF}$ , which has the same overall effect as reducing the abscissa.

The approach used to determine if there are benefits to internal only cooling when TBCs are used can be summarized as follows:

- 1) Choose coolant temperature ratio,  $T_C/T_G$ , maximum metal temperature ratio,  $T_M/T_G$ , and  $k/t$  values for both the metal and TBC.
- 2) Choose external heat transfer coefficients at different Reynolds numbers for both solid and film cooled vanes.
- 3) Choose effectiveness values for the film cooled vane.
- 4) Calculate external and internal surface temperatures for solid and film cooled vanes with and without a TBC.
- 5) Calculate the internal heat transfer coefficients for film cooled vane, and reduced heat transfer coefficients due to cross-flow for an internal only cooled vane.
- 6) Determine the required  $x/d$  for an internal unit Reynolds number of  $250,000\text{cm}^{-1}$ , and for this  $x/d$  determine the required coolant flow rate for the entire vane surface.
- 7) Determine the coolant-to-mainstream flow rates for the different conditions.

#### Comparison of TBC and metal vane heat transfer.

Fixed metal outer surface temperature. The choice of film cooled or only internal cooling for TBC coated vanes is dependent on specific applications. To illustrate a framework for making cooling choices, it is helpful to choose a specific vane geometry. To maintain the focus on the issues of film cooling and coatings a simple two-dimensional flow case is used. Because data are available that illustrate several of the factors affecting external heat transfer for film cooling in references 5 and 6, this vane geometry is chosen. Where available, data at the highest turbulence intensity, (6%), are used. The data at lower turbulence intensities show internal only cooling in a more favorable light, but are not as representative of engine vane inlet conditions. While these references have data at different exit Mach numbers, only the 0.9 Mach number data are used here.

Table II summarizes the comparison between film and non-film cooling for metal only designs and designs using a TBC coated vane. The vane surface is divided into three somewhat arbitrary regions. The leading edge region is between the first row of coolant holes on the pressure surface and the first row of holes on the suction surface. Film cooling in this region was based on the results of Ekkad et al.[14]. The heat transfer coefficient was increased by nearly 20% over the non-film cooled data. The film cooling flow rate was scaled from the experimental data. The leading edge region was 18% of the total surface area. The suction surface region is from the cooling holes to the trailing edge. This distance is 140 hole diameters, and 46% of the total surface distance. Similarly, the pressure surface distance is from the cooling holes to the trailing edge. This distance is 110 hole diameters, (36%), of the total surface

Table II. Average coolant flows

| a) Internal only cooling  |            |       |       |       |
|---------------------------|------------|-------|-------|-------|
|                           | Metal only |       | TBC   |       |
| $Re_{2-C} \times 10^{-6}$ | 1.0        | 2.0   | 1.0   | 2.0   |
| Surface                   |            |       |       |       |
| Leading edge              |            |       |       |       |
| $h_O, W/m^2K$             | 5990       | 4429  | 5990  | 4429  |
| $s, mm$                   | 27         | 27    | 27    | 27    |
| $T_S/T_G$                 | 0.7        | 0.7   | 0.893 | 0.871 |
| $h_I, W/m^2K$             | 15898      | 9790  | 3800  | 3310  |
| $T_I/T_G$                 | 0.613      | 0.636 | 0.669 | 0.672 |
| Coolant ratio, %          | 4.93       | 1.82  | 0.26  | 0.22  |
| Suction surface           |            |       |       |       |
| $h_O, W/m^2K$             | 5131       | 4694  | 5131  | 4694  |
| $s, mm$                   | 70         | 70    | 70    | 70    |
| $T_S/T_G$                 | 0.7        | 0.7   | 0.882 | 0.875 |
| $h_I, W/m^2K$             | 12263      | 10678 | 3550  | 3402  |
| $T_I/T_G$                 | 0.626      | 0.632 | 0.671 | 0.672 |
| Coolant ratio, %          | 7.50       | 5.64  | 0.59  | 0.54  |
| Pressure surface          |            |       |       |       |
| $h_O, W/m^2K$             | 4100       | 4247  | 4100  | 4247  |
| $s, mm$                   | 55         | 55    | 55    | 55    |
| $T_S/T_G$                 | 0.7        | 0.7   | 0.865 | 0.868 |
| $h_I, W/m^2K$             | 8754       | 9210  | 3179  | 3238  |
| $T_I/T_G$                 | 0.641      | 0.638 | 0.673 | 0.673 |
| Coolant ratio, %          | 2.96       | 3.27  | 0.37  | 0.38  |
| Total                     |            |       |       |       |
| Coolant ratio, %          | 15.39      | 10.73 | 1.22  | 1.14  |

distance. The coolant ratio is the amount of coolant required per unit span divided by the main flow rate per unit span,  $(\rho V)_{IN}P$ .

Calculations were done with a impingement diameter of 0.5mm. All coolant flow rates were calculated assuming no cross flow. At these temperatures the metal only calculations which included cross flow correction resulted in extremely high flow rates, and more importantly, impractical impingement array parameters. To accommodate cross flow the jet diameters were extremely large.

The external heat transfer coefficients in Table II are based on the experimental Nusselt numbers and a thermal conductivity at  $2000^\circ K$ . The  $h_I$  values are calculated to maintain a maximum metal temperature of  $1400^\circ K$ . The internal heat transfer coefficients are calculated using the conductivity of air at  $1000^\circ K$ .

Table IIa shows nearly a ten fold reduction in coolant flow rates when a TBC is used. This is primarily due to an increase in the surface temperature when a TBC is used. This results in lower vane heat fluxes. Consequently, the metal inner wall temperatures increase, which results in lowered required internal heat transfer coefficients.

Table II concluded

Table III. Fixed TBC temperature coolant flows

| b) Film and internal cooling |            |       |       |       |
|------------------------------|------------|-------|-------|-------|
| $Re_{2-C} \times 10^{-6}$    | Metal only |       | TBC   |       |
|                              | 1.0        | 2.0   | 1.0   | 2.0   |
| Surface                      |            |       |       |       |
| Leading edge                 |            |       |       |       |
| $h_O, W/m^2 K$               | 7214       | 5315  | 7214  | 5315  |
| $\eta$                       | 0.1        | 0.1   | 0.1   | 0.1   |
| $\phi$                       | 0.6        | 0.6   | 0.258 | 0.294 |
| $h_{O-EFF}, W/m^2 K$         | 6012       | 4429  | 4422  | 3504  |
| $s, mm$                      | 27         | 27    | 27    | 27    |
| $T_S/T_G$                    | 0.7        | 0.7   | 0.871 | 0.853 |
| $h_I, W/m^2 K$               | 16001      | 9790  | 3307  | 2923  |
| $T_I/T_G$                    | 0.613      | 0.636 | 0.672 | 0.675 |
| Coolant ratio, internal, %   | 4.94       | 1.80  | 0.20  | 0.15  |
| Coolant ratio, film, %       | 0.36       | 0.36  | 0.36  | 0.36  |
| Suction surface              |            |       |       |       |
| $h_O, W/m^2 K$               | 7039       | 5911  | 7039  | 5911  |
| $\eta$                       | 0.1        | 0.1   | 0.1   | 0.1   |
| $\phi$                       | 0.6        | 0.6   | 0.261 | 0.280 |
| $h_{O-EFF}, W/m^2 K$         | 5866       | 4925  | 4344  | 3801  |
| $s, mm$                      | 70         | 70    | 70    | 70    |
| $T_S/T_G$                    | 0.7        | 0.7   | 0.869 | 0.860 |
| $h_I, W/m^2 K$               | 15324      | 11500 | 3276  | 3056  |
| $T_I/T_G$                    | 0.615      | 0.629 | 0.673 | 0.674 |
| Coolant ratio, internal, %   | 11.73      | 6.50  | 0.50  | 0.43  |
| Coolant ratio, film, %       | 1.57       | 1.57  | 1.57  | 1.57  |
| Pressure surface             |            |       |       |       |
| $h_O, W/m^2 K$               | 4208       | 3991  | 4208  | 3991  |
| $\eta$                       | 0.1        | 0.1   | 0.1   | 0.1   |
| $\phi$                       | 0.6        | 0.6   | 0.321 | 0.328 |
| $h_{O-EFF}, W/m^2 K$         | 3507       | 3326  | 2899  | 2774  |
| $s, mm$                      | 55         | 55    | 55    | 55    |
| $T_S/T_G$                    | 0.7        | 0.7   | 0.839 | 0.836 |
| $h_I, W/m^2 K$               | 7054       | 6577  | 2619  | 2549  |
| $T_I/T_G$                    | 0.649      | 0.652 | 0.678 | 0.678 |
| Coolant ratio, internal, %   | 1.88       | 1.63  | 0.25  | 0.23  |
| Coolant ratio, film, %       | 0.31       | 0.31  | 0.31  | 0.31  |
| Total                        |            |       |       |       |
| Coolant ratio, internal, %   | 18.55      | 9.93  | 0.95  | 0.81  |
| Coolant ratio, film, %       | 2.24       | 2.24  | 2.24  | 2.24  |
| Overall coolant ratio, %     | 22.20      | 12.17 | 3.19  | 3.05  |

The metal only total cooling flows in Table IIa are between 10 and 15% of the mainstream flow. These flow ratios are too high to be ejected from the trailing edge. Thulin et al.[24] in their design for a high pressure turbine had less than 2% of the mainstream air ejected from the trailing edge. The required coolant when TBC's are used is less than 2% of the mainstream flow.

Comparing Table IIa and Table IIb for the metal only vane shows a large amount of internal cooling is required, even with film cooling. In practice, additional cooling rows would be added to reduce the required internal cooling. When the film cooling flows are added to the internal flows, internal only cooling results in lower coolant flow rates. Film cooling causes laminar boundary layers to become

| a) Internal only cooling  |       |       |       |       |       |       |
|---------------------------|-------|-------|-------|-------|-------|-------|
| $T_{MO}/T_G$              | 0.700 |       | 0.725 |       | 0.700 |       |
| $T_C/T_G$                 | 0.500 |       | 0.500 |       | 0.475 |       |
| $Re_{2-C} \times 10^{-6}$ | 1.0   | 2.0   | 1.0   | 2.0   | 1.0   | 2.0   |
| Surface                   |       |       |       |       |       |       |
| Leading edge              |       |       |       |       |       |       |
| $h_O, W/m^2 K$            | 5990  | 4429  | 5990  | 4429  | 5990  | 4429  |
| $s, mm$                   | 27    | 27    | 27    | 27    | 27    | 27    |
| $T_S/T_G$                 | 0.775 | 0.775 | 0.800 | 0.800 | 0.775 | 0.775 |
| $h_I, W/m^2 K$            | 9987  | 6570  | 7166  | 4859  | 8411  | 5487  |
| $T_I/T_G$                 | 0.635 | 0.652 | 0.667 | 0.682 | 0.660 | 0.678 |
| $w_C, \%$                 | 1.90  | 0.80  | 0.96  | 0.43  | 1.34  | 0.56  |
| Suction surface           |       |       |       |       |       |       |
| $h_O, W/m^2 K$            | 5131  | 4694  | 5131  | 4694  | 5131  | 4694  |
| $s, mm$                   | 70    | 70    | 70    | 70    | 70    | 70    |
| $T_S/T_G$                 | 0.775 | 0.775 | 0.800 | 0.800 | 0.775 | 0.775 |
| $h_I, W/m^2 K$            | 8005  | 7083  | 5848  | 5222  | 6677  | 5956  |
| $T_I/T_G$                 | 0.644 | 0.649 | 0.675 | 0.680 | 0.670 | 0.675 |
| $w_C, \%$                 | 3.12  | 2.43  | 1.64  | 1.30  | 2.16  | 1.71  |
| Pressure surface          |       |       |       |       |       |       |
| $h_O, W/m^2 K$            | 4100  | 4247  | 4100  | 4247  | 4100  | 4247  |
| $s, mm$                   | 55    | 55    | 55    | 55    | 55    | 55    |
| $T_S/T_G$                 | 0.775 | 0.775 | 0.800 | 0.800 | 0.775 | 0.775 |
| $h_I, W/m^2 K$            | 5930  | 6208  | 4418  | 4615  | 5075  | 5260  |
| $T_I/T_G$                 | 0.655 | 0.654 | 0.685 | 0.684 | 0.681 | 0.679 |
| $w_C, \%$                 | 1.33  | 1.45  | 0.72  | 0.79  | 0.97  | 1.04  |
| Total                     |       |       |       |       |       |       |
| $w_C, \%$                 | 6.36  | 4.68  | 3.32  | 2.52  | 4.47  | 3.31  |

turbulent. Comparisons at Reynolds numbers of 1 and 2 million indicate that at higher Reynolds numbers the penalty associated with early boundary layer transition would be less.

Comparisons of Table IIa and Table IIb for the TBC vanes leads to a different conclusion. With film cooling, the internal cooling ratio is consistently lower than for the non film cooled results. However, the film cooling flow rate is more than twice the internal only coolant. Overall, the total coolant flow rate with film cooling is nearly three times as great as the non-film cooled flow rate at both Reynolds number. This indicates that at high Reynolds numbers internal only cooling may still be preferred.

Since the internal cooling flow rates were much less with a TBC coating, the increase in internal cooling after accounting for cross flow was not large. On average, the increase in internal cooling flows was 20% or less. If the increase in cooling due to cross flows had been included in Table IIa, the total cooling ratio would still be less than 1.5% for a TBC coating.

**Fixed TBC outer surface temperature.** The primary reason for the low cooling rates associated with the reliance on TBC coatings is the high surface temperatures, where  $T_S/T_G$  is in the range of 0.860 to 0.882. For  $T_G = 2000^\circ K$ , surface temperatures exceed  $1720^\circ K$ . While these temperatures are close to the future goals for TBC surface temperatures, they are significantly higher than current



Table III concluded

| b) Film and internal cooling |       |       |       |       |       |       |
|------------------------------|-------|-------|-------|-------|-------|-------|
| $T_{MO}/T_G$                 | 0.700 |       | 0.725 |       | 0.700 |       |
| $T_C/T_G$                    | 0.500 |       | 0.500 |       | 0.475 |       |
| $Re_{2-C} \times 10^{-6}$    | 1.0   | 2.0   | 1.0   | 2.0   | 1.0   | 2.0   |
| Surface                      |       |       |       |       |       |       |
| Leading edge                 |       |       |       |       |       |       |
| $h_O, W/m^2 K$               | 7214  | 5315  | 7214  | 5315  | 7214  | 5315  |
| $\eta$                       | 0.1   | 0.1   | 0.1   | 0.1   | 0.1   | 0.1   |
| $\phi$                       | 0.450 | 0.450 | 0.400 | 0.400 | 0.429 | 0.429 |
| $h_{O-EFF}, W/m^2 K$         | 5611  | 4134  | 5411  | 3987  | 5504  | 4069  |
| $s, mm$                      | 27    | 27    | 27    | 27    | 27    | 27    |
| $T_S/T_G$                    | 0.775 | 0.775 | 0.800 | 0.800 | 0.775 | 0.775 |
| $h_I, W/m^2 K$               | 9088  | 5993  | 6262  | 4271  | 7345  | 5035  |
| $T_I/T_G$                    | 0.639 | 0.655 | 0.673 | 0.686 | 0.666 | 0.681 |
| Internal $w_C, \%$           | 1.55  | 0.66  | 0.72  | 0.33  | 1.00  | 0.46  |
| Film $w_{rMC}, \%$           | 0.36  | 0.36  | 0.36  | 0.36  | 0.36  | 0.36  |
| Suction surface              |       |       |       |       |       |       |
| $h_O, W/m^2 K$               | 7039  | 5911  | 7039  | 5911  | 7039  | 5911  |
| $\eta$                       | 0.1   | 0.1   | 0.1   | 0.1   | 0.1   | 0.1   |
| $\phi$                       | 0.450 | 0.450 | 0.400 | 0.400 | 0.429 | 0.429 |
| $h_{O-EFF}, W/m^2 K$         | 5475  | 4598  | 5280  | 4433  | 5378  | 4520  |
| $s, mm$                      | 70    | 70    | 70    | 70    | 70    | 70    |
| $T_S/T_G$                    | 0.775 | 0.775 | 0.800 | 0.800 | 0.775 | 0.775 |
| $h_I, W/m^2 K$               | 8772  | 6891  | 6065  | 4868  | 7162  | 5727  |
| $T_I/T_G$                    | 0.640 | 0.650 | 0.674 | 0.682 | 0.667 | 0.676 |
| Internal $w_C, \%$           | 3.73  | 2.27  | 1.75  | 1.11  | 2.47  | 1.56  |
| Film $w_C, \%$               | 1.57  | 1.57  | 1.57  | 1.57  | 1.57  | 1.57  |
| Pressure surface             |       |       |       |       |       |       |
| $h_O, W/m^2 K$               | 4208  | 3991  | 4208  | 3991  | 4208  | 3991  |
| $\eta$                       | 0.1   | 0.1   | 0.1   | 0.1   | 0.1   | 0.1   |
| $\phi$                       | 0.450 | 0.450 | 0.400 | 0.400 | 0.429 | 0.429 |
| $h_{O-EFF}, W/m^2 K$         | 3273  | 3104  | 3156  | 2994  | 3204  | 3048  |
| $s, mm$                      | 55    | 55    | 55    | 55    | 55    | 55    |
| $T_S/T_G$                    | 0.775 | 0.775 | 0.800 | 0.800 | 0.775 | 0.775 |
| $h_I, W/m^2 K$               | 4473  | 4191  | 3051  | 2549  | 3695  | 3525  |
| $T_I/T_G$                    | 0.664 | 0.666 | 0.695 | 0.696 | 0.691 | 0.692 |
| Internal $w_C, \%$           | 0.74  | 0.64  | 0.38  | 0.34  | 0.50  | 0.45  |
| Film $w_C, \%$               | 0.31  | 0.31  | 0.31  | 0.31  | 0.31  | 0.31  |
| Total                        |       |       |       |       |       |       |
| Internal $w_C, \%$           | 5.02  | 3.57  | 2.85  | 1.78  | 3.97  | 2.47  |
| Film $w_C, \%$               | 2.24  | 2.24  | 2.24  | 2.24  | 2.24  | 2.24  |
| Overall $w_C, \%$            | 7.26  | 5.81  | 5.09  | 4.02  | 6.21  | 4.71  |

TBC values. To address this issue, the calculations were repeated with the TBC outer surface temperature, as well as the outer metal temperature held constant. The thermal resistance of the TBC was allowed to decrease in order to lower the temperature drop across the TBC. Table III shows the sensitivity of cooling flows to temperature changes. Miller[27] gives a near term temperature capability goal for TBC coatings of  $1550^\circ K$ . For  $T_G = 2000^\circ K$ , the value for  $T_S/T_G$  is 0.775. Comparing the last two columns of Table II for the TBC coating, with the first two columns of Table III shows that holding  $T_S/T_G = 0.775$  increases the required cooling flows by between three and five percent of the mainstream flow. However, the relative advantage of not using film cooling remains, even though it is reduced from nearly two percent of mainflow air to about one percent of mainflow air.

Table III shows that allowing the outer metal temperature ratio,  $T_{MO}/T_G$ , to increase from 0.700 to 0.725, and maintaining the same temperature drop across the TBC coating results in less required coolant. More importantly, comparing parts a and b shows that the total required coolant air is reduced by more than 1.5%, when no film cooling is used. The rates of 2.5 to 3.3% are low enough that they could be ejected from the trailing edge.

Comparing the first two and last two columns in Table III shows that a  $50^\circ$  decrease in coolant supply temperature decreases the required coolant by about one percent when film cooling is used. When no film cooling is used, the decrease is greater, approaching two percent at the lower Reynolds number.

## CONCLUDING REMARKS

An analysis of the sensitivity of NOx production to cooling flow rates showed that even a small reduction in vane cooling can significantly reduce NOx production. Halving the vane cooling flow rate from ten to five percent may reduce NOx by twenty five percent.

An analysis of the effects of TBC coatings on the required vane cooling flows showed that internal only cooling may be appropriate for designs relying on the TBC to maintain a maximum metal temperature. For low vane Reynolds numbers, associated with small vane sizes, internal only cooling is attractive because the early transition to turbulence due to the cooling holes may be avoided. With a TBC the sensitivity of cooling flows to Reynolds number was less than for the metal only assumption.

Overall, the calculations using the GlennHT code were a reasonably good predictor of heat transfer changes due to film cooling. If film cooling is not used, there is a need for accurate transition modeling, when predicting blade heat transfer. Also, there is a need for modeling to account for the effects of freestream turbulence on heat transfer, especially when the flow is laminar. Designing a flow path that delays transition is especially beneficial for internal only cooling approaches.

Even though internal only cooling flow rates were less than the film cooling rates for metal vanes, the internal only cooling flow rates were still high, and their implementation was impractical. With a TBC internal only cooling becomes practical due to the much lower flow rates. Improving film cooling effectiveness would reduce the relative advantage of internal only cooling using a TBC. Internal only cooling also minimizes the possibility of unburned fuel burning on the vane surface due to the oxygen rich unburned cooling air. However, if the blowing ratio could be reduced, without increasing the possibility of hot gas ingestion, the relative advantage of internal only cooling would decrease.

The analysis presented in this work was focused on the effects of relying on a TBC from the standpoint of cooling flow requirements. Because of the large reduction in cooling requirements when relying on a TBC, internal only may be attractive. Whether internal only or film cooling or a combination of both is used depends on the specific application.

## REFERENCES

1. Lefebvre, A.H., 1998, *Gas Turbine Combustion*, Second edition, Taylor & Francis, Inc., New York.
2. Reed, J.A., Turner, M.G., 2005, "An Entropy Loss Approach for a Meanline Bladerow Model with Coupling to Test Data and 3D CFD Results," ASME paper GT2005-68608
3. Wilcock, R.C., Young, J.B., and Horlock, J.H., 2005, "The Effect of Turbine Blade Cooling on the Cycle Efficiency of Gas Turbine Power Cycles," ASME *Journal of Engineering for Gas Turbines and Power*, Vol. 127, pp. 109-120.
4. MacArthur, C.D., 1999, "Advanced Aero-Engine Turbine Technologies and Their Application to Industrial Gas Turbines," *ISABE: 14th Int. Symp. on Air-Breathing Engines*, Florence, Italy, Paper 99-7151.
5. Arts, T., Lambert de Rouvroit, M., and Rutherford, A.W., 1990, "Aero-Thermal Investigation of a Highly Loaded Transonic Linear Turbine Guide Vane Cascade," VKI Technical Note 174.
6. Arts, T., 1995, "Thermal Investigation of a Highly Loaded Transonic Turbine Film Cooled Guide Vane", 1<sup>st</sup> European Conf. on Turbomachinery - Fluid Dynamic and Thermodynamic Aspects, Erlanger, Germany, also VKI preprint 1995-11.
7. Shuman, T.R., 2000, "NOx and CO Formation for Lean-Premixed Methane-Air Combustion in a Jet-Stirred Reactor Operated at Elevated Temperatures," PhD Thesis, Mech. Engr. Dept., Univ. of Washington.
8. Mello, J.P., Mellor, A.M., Steele, R.C., and Smith, K.O., 1997, "A Study of the Factors Affecting NOx Emissions in Lean Premixed Turbine Combustors," AIAA paper AIAA-1997-2708.
9. Tacina, R., Wey, C., Laing, P., and Mansour, A., 2002, "A Low NOx Lean-Direct Injection, Multipoint Integrated Module Combustor Concept for Advanced Aircraft Gas Turbines," NASA TM-2002-211347, Presented at the Conference on Technologies and Combustion for a Clean Environment, Oporto, Portugal, July 2001.
10. Nealy, D.A., Mihlec, M.S., Hylton, L.D., and Gladden, H.J., 1984, "Measurements of Heat Transfer Distribution Over the Surfaces of Highly Loaded Turbine Nozzle Guide Vanes," ASME *Journal of Engineering for Gas Turbines and Power*, Vol. 106, pp. 149-158.
11. Radomsky, R. W., and Thole, K.A., 2002, "Detailed Boundary Layer Measurements on a Stator Vane at Elevated Freestream Turbulence Levels," *Journal of Turbomachinery*, Vol. 124, pp. 107-118.
12. Harasgama, S.P., and Wedlake, E.T., 1991, "Heat Transfer and Aerodynamics of a High Rim Speed Turbine Nozzle Guide Vane Tested in the RAE Isentropic Light Piston Cascade (ILPC)," *Journal of Turbomachinery*, Vol. 113, pp. 384-391.
13. Giel, P.W., Van Fossen, G.J., Boyle, R.J., Thurman, D.R., and Civinskas, K.C., 1999, "Blade Heat Transfer Measurements and Predictions in a Transonic Turbine Cascade," ASME paper 99-GT-125.
14. Ekkad, S.V., Han, J.C., and Du, H., 1998, "Detailed Film Cooling Measurements on a Cylindrical Leading Edge Model: Effect of Free-Stream Turbulence and Coolant Density," ASME *Journal of Turbomachinery*, Vol. 120, pp. 799-807.
15. Garg, V.K., 2002, "Heat transfer research on gas turbine airfoils at NASA GRC," *International Journal of Heat and Fluid Flow*, Vol. 23, pp. 109-136.
16. Steinthorson, E., Ameri, A.A., Rigby, D.L., 1997, "TRAF3D.MB- A Multi-block Flow Solver for Turbomachinery Flows," AIAA paper 97-0996.
17. Schiele, R., Sieger, K., Schulz, A., and Wittig, S., 1995, "Heat Transfer Investigations on a Highly Loaded Aerothermally Designed Turbine Cascade" ISABE paper 95-7100.
18. Boyle, R.J., Giel, P.W., and Ames, F.E., "Predictions for the Effects of Freestream Turbulence on Turbine Blade Heat Transfer," ASME paper GT2004-54332.
19. Bons, J.P., MacArthur, C.D., and River, R.B., 1996, "The Effect of High Free-Stream Turbulence on Film Cooling Effectiveness," ASME *Journal of Turbomachinery*, Vol. 118, pp. 814-825.
20. Takeishi, K., Matsuura, M., Aoki, S., and Sato, T., 1990, "An Experimental Study of Heat Transfer and Film Cooling on Low Aspect Ratio Turbine Nozzles," ASME *Journal of Turbomachinery*, Vol. 112, pp. 488-496.
21. Drost, U., and Bolcs, A., 1999, "Investigation of Detailed Film Cooling Effectiveness and Heat Transfer Distributions on a Gas Turbine Airfoil," ASME *Journal of Turbomachinery*, Vol. 121, pp. 233-242.
22. Han, J. C., Dutta, S, and Ekkad, S.V., 2000, "*Gas Turbine Heat Transfer and Cooling Technology*," Taylor & Francis Inc., New York.
23. Zhu, D., Miller, R.A., 2000, "Thermal Conductivity and Elastic Modulus Evolution of Thermal Barrier Coatings under High Heat Flux Conditions," *Journal of Thermal Spray Technology*, Vol. 9, No. 2, pp. 175-180.
24. Special Metals web site - [www.specialmetals.com](http://www.specialmetals.com)
25. Thulin, R.D., Howe, D.C., and Singer, I.D., 1982, "Energy Efficiency Engine High Pressure Detailed Design Report," NASA CR-165680, also PWA-5594-171
26. Florschuetz, L.W., Truman, C.R., and Metzger, D.E., 1981, "Streamwise Flow and Heat Transfer Distributions for Jet Array Impingement with Crossflow," *Journal of Heat Transfer*, Vol. 103, pp. 337-342.
27. Miller, R., 2006, Private Communication.

## Appendix A

### Ratio of coolant flows with and without extraction

Without film cooling the one dimensional heat balance is given by:

$$h_O(T_G - T_{TBCO}) = (k/t)_{TBC}(T_{TBCO} - T_{TBCI})$$

$$(k/t)_{TBC}(T_{TBCO} - T_{TBCI}) = (k/t)_M(T_{TBCI} - T_{TMI})$$

$$(k/t)_M(T_{TBCI} - T_{TMI}) = h_I(T_{TMI} - T_C)$$

$T_G$  is the design gas temperature, and is typically greater than  $T_{40}$  after accounting for a pattern factor, and a recovery factor. Values are assumed for  $h_O/(k/t)_M$ ,  $(k/t)_{TBC}/(k/t)_M$ ,  $T_C/T_G$ , and  $T_{TBCI}/T_G$ , where  $T_{TBCI}$  is also the maximum metal temperature. The equations are solved for the remaining temperatures and  $h_I/(k/t)_M$ .

Han, Dutta, and Ekkad [21] showed that, for a variety of internal cooling schemes, the Nusselt number is proportional to the Reynolds number to a power,  $n$ , with  $0.65 \leq n \leq 0.75$ . Since the Reynolds number is directly proportional to the internal cooling flow rate,

$$w_C \propto h_I^{1/n}$$

When film cooling is used,  $T_G$  is replaced by the adiabatic wall temperature  $T_{AW}$ , which is found from the film effectiveness.

The beneficial effects of film cooling are offset to some degree by an increase in  $h_O$ . If using film cooling causes a laminar boundary layer to become turbulent, the increase in  $h_O$  can be substantial.

When film cooling is used there is an additional penalty to the cooling flow rates. Not all the cooling air is available for internal cooling. If all of the coolant is extracted for film cooling, the average internal coolant flow is reduced by half. The ratio of coolant required with film cooling to the coolant required with only internal cooling is:

$$\frac{w_{C-Film}}{w_{C-NoFilm}} = \left( \frac{h_{I-Film}}{h_{I-NoFilm}} \right)^{1/n} \left( \frac{1}{1 - 0.5w_{C-EXT}/w_{C-Film}} \right)$$

$w_{C-EXT}/w_{C-Film}$  is the fraction of film cooling extracted through the film cooling holes.

The results in figure 5 were generated assuming  $n = 0.75$ . This high value for  $n$  gives a conservative value for  $w_{C-Film}/w_{C-NoFilm}$ .

**REPORT DOCUMENTATION PAGE**

*Form Approved*  
OMB No. 0704-0188

The public reporting burden for this collection of information is estimated to average 1 hour per response, including the time for reviewing instructions, searching existing data sources, gathering and maintaining the data needed, and completing and reviewing the collection of information. Send comments regarding this burden estimate or any other aspect of this collection of information, including suggestions for reducing this burden, to Department of Defense, Washington Headquarters Services, Directorate for Information Operations and Reports (0704-0188), 1215 Jefferson Davis Highway, Suite 1204, Arlington, VA 22202-4302. Respondents should be aware that notwithstanding any other provision of law, no person shall be subject to any penalty for failing to comply with a collection of information if it does not display a currently valid OMB control number.

PLEASE DO NOT RETURN YOUR FORM TO THE ABOVE ADDRESS.

|   |                         |   |                                   |   |   |
|---|-------------------------|---|-----------------------------------|---|---|
| <b>1. REPORT DATE (DD-MM-YYYY)</b><br>01-12-2007  |                         | <b>2. REPORT TYPE</b><br>Technical Memorandum |                                   | <b>3. DATES COVERED (From - To)</b>   |   |
| <b>4. TITLE AND SUBTITLE</b><br>Effects of Thermal Barrier Coatings on Approaches to Turbine Blade Cooling  |                         |   |                                   | <b>5a. CONTRACT NUMBER</b>  |   |
|   |                         |   |                                   | <b>5b. GRANT NUMBER</b>   |   |
|   |                         |   |                                   | <b>5c. PROGRAM ELEMENT NUMBER</b>   |   |
| <b>6. AUTHOR(S)</b><br>Boyle, Robert, J.  |                         |   |                                   | <b>5d. PROJECT NUMBER</b>   |   |
|   |                         |   |                                   | <b>5e. TASK NUMBER</b>  |   |
|   |                         |   |                                   | <b>5f. WORK UNIT NUMBER</b><br>WBS 561581.02.01.03.08                               |   |
| <b>7. PERFORMING ORGANIZATION NAME(S) AND ADDRESS(ES)</b><br>National Aeronautics and Space Administration<br>John H. Glenn Research Center at Lewis Field<br>Cleveland, Ohio 44135-3191  |                         |   |                                   | <b>8. PERFORMING ORGANIZATION REPORT NUMBER</b><br>E-16110                          |   |
| <b>9. SPONSORING/MONITORING AGENCY NAME(S) AND ADDRESS(ES)</b><br>National Aeronautics and Space Administration<br>Washington, DC 20546-0001  |                         |   |                                   | <b>10. SPONSORING/MONITORS ACRONYM(S)</b><br>NASA                                   |   |
|   |                         |   |                                   | <b>11. SPONSORING/MONITORING REPORT NUMBER</b><br>NASA/TM-2007-214933; GT2006-91202 |   |
| <b>12. DISTRIBUTION/AVAILABILITY STATEMENT</b><br>Unclassified-Unlimited<br>Subject Category: 34<br>Available electronically at <a href="http://gltrs.grc.nasa.gov">http://gltrs.grc.nasa.gov</a><br>This publication is available from the NASA Center for AeroSpace Information, 301-621-0390   |                         |   |                                   |   |   |
| <b>13. SUPPLEMENTARY NOTES</b>  |                         |   |                                   |   |   |
| <b>14. ABSTRACT</b><br>Reliance on Thermal Barrier Coatings (TBC) to reduce the amount of air used for turbine vane cooling is beneficial both from the standpoint of reduced NOx production, and as a means of improving cycle efficiency through improved component efficiency. It is shown that reducing vane cooling from 10 to 5 percent of mainstream air can lead to NOx reductions of nearly 25 percent while maintaining the same rotor inlet temperature. An analysis is given which shows that, when a TBC is relied upon in the vane thermal design process, significantly less coolant is required using internal cooling alone compared to film cooling. This is especially true for small turbines where internal cooling without film cooling permits the surface boundary layer to remain laminar over a significant fraction of the vane surface. |                         |   |                                   |   |   |
| <b>15. SUBJECT TERMS</b><br>Heat transfer; Turbine cooling  |                         |   |                                   |   |   |
| <b>16. SECURITY CLASSIFICATION OF:</b>  |                         |   | <b>17. LIMITATION OF ABSTRACT</b> | <b>18. NUMBER OF PAGES</b><br>21  | <b>19a. NAME OF RESPONSIBLE PERSON</b><br>STI Help Desk (email:help@sti.nasa.gov) |
| <b>a. REPORT</b><br>U   | <b>b. ABSTRACT</b><br>U | <b>c. THIS PAGE</b><br>U                      |                                   |   | UU  |



